The dependence on temperature and salinity of dissolved

Bakker, Dorothee C.E.; Baar, Hein J.W. de; Jong, Edwin de

Published in:
Marine Chemistry

DOI:
10.1016/S0304-4203(99)00017-1

ELSEVIER

Marine Chemistry 65 (1999) 263–280

MARINE CHEMISTRY

The dependence on temperature and salinity of dissolved inorganic carbon in East Atlantic surface waters

Dorothee C.E. Bakker *, Hein J.W. de Baar [1], Edwin de Jong

Netherlands Institute for Sea Research, P.O. Box 59, 1790 AB Den Burg, Texel, Netherlands

Received 19 June 1998; accepted 26 January 1999

Abstract

Recurring latitudinal patterns of the dissolved inorganic carbon (DIC) content and the fugacity of CO_2 (fCO_2) were observed in East Atlantic surface waters with strong gradients at hydrographic fronts. The dissolved inorganic carbon chemistry clearly displayed the effects of oceanic circulation and of persistent surface water processes. In two cases inorganic carbon components could be used as an indicator of the origin of hydrographic features. Surface water fCO_2 below the atmospheric value, low DIC and low salinity north of the equator were ascribed to a combination of high rainfall and low wind speed in the Intertropical Convergence Zone and of biological uptake of CO_2. Low surface water DIC and salinity delineated the Congo outflow. Along the cruise tracks calculated titration alkalinity (TA) had an almost linear relationship with salinity, while DIC had an apparent dependence on temperature and salinity. The latter dependence was tested by comparing observed DIC to DIC estimated from fCO_2 and a reference value of TA normalised to salinity. Different scenarios of temperature, salinity, fCO_2 and nutrient contents were applied. Changes of DIC were found to be indeed related to both temperature and salinity. The latitudinal distribution of DIC could be inferred with an accuracy of 17 μmol kg^{-1} and a standard deviation of 13 μmol kg^{-1} from in situ salinity, in situ temperature and the reference values of TA and nutrient contents normalised to in situ salinity (scenario D). The applied technique of estimating DIC from temperature and salinity is a powerful diagnostic tool to evaluate the spatial distribution of DIC.

Keywords: dissolved inorganic carbon; East Atlantic Ocean; salinity; temperature

1. Introduction

The continuing increase of the atmospheric content of the greenhouse gas carbon dioxide (CO_2) may give rise to global warming (Houghton et al., 1996). Estimates of the net oceanic uptake of CO_2 contain a large uncertainty as a result of the large natural air–sea exchange of CO_2, which has a considerable spatial and temporal variability. Worldwide measurements of surface water CO_2-characteristics and of the related air–sea exchange of CO_2 are being made in order to better assess the oceanic uptake of CO_2 (Poisson et al., 1993; Takahashi et al., 1993, 1997; among others). In this context it is important to understand the processes that affect the

* Corresponding author. School of Environmental Sciences, University of East Anglia, Norwich NR4 7TJ, UK. Tel.: +44-1603-593763; Fax: +44-1603-507719; E-mail: d.bakker@uea.ac.uk

[1] Tel.: +31-222-369465; Fax: +31-222-319674; E-mail: debaar@nioz.nl

0304-4203/99/$ - see front matter
PII: S0304-4203(99)00017-1

Table 1
Surface water parameters for the cruises ANT XI/1 and XI/5 of R.V. *Polarstern*

	ANT XI/1	ANT XI/5
Ports	Bremerhaven—Capetown	Capetown—Rotterdam
Period	18 October–27 November 1993	21 May–15 June 1994
Temperature	on-line	on-line
Salinity	on-line	on-line
fCO_2	on-line	on-line
DIC	on-line	on-line
TA	calculated	calculated
$Si(OH)_4$	discrete	discrete
NO_3^-	discrete	discrete
PO_4^{3-}	discrete	none
'Relative chlorophyll' (XI/1), fluorescence (XI/5)	on-line	on-line

The fugacity of CO_2 (fCO_2), dissolved inorganic carbon (DIC), contents of silicate ($Si(OH)_4$), nitrate (NO_3^-) and phosphate (PO_4^{3-}) were determined either on-line or for discrete samples. Titration alkalinity (TA) was calculated from DIC and fCO_2. Measurements of 'relative chlorophyll' (XI/1) and fluorescence (XI/5) were not calibrated.

distribution of dissolved inorganic carbon (DIC) components in oceanic surface waters.

DIC in seawater consists of roughly 0.5 to 1% CO_2, 0.002% carbonic acid (H_2CO_3), 90% bicarbonate (HCO_3^-) and 9% carbonate (CO_3^{2-}):

$$\mathrm{DIC} = [CO_2] + [H_2CO_3] + [HCO_3^-] + [CO_3^{2-}] \quad (1)$$

The fugacity of CO_2, fCO_2 (μatm), is the ratio of the concentration of dissolved CO_2 in seawater $[CO_{2T}]$, which includes the negligible amount of carbonic acid, to its solubility K_0' (mol kg^{-1} atm^{-1}) (Weiss, 1974):

$$fCO_2 = [CO_{2T}]/K_0' \quad (2)$$

An increase in temperature or salinity would decrease the solubility of CO_2. The titration alkalinity (TA, μeq kg^{-1}) is the equivalent of all bases that can accept a proton to the carbonic acid endpoint (Sverdrup et al., 1942; Dickson, 1981):

$$\mathrm{TA} = [HCO_3^-] + 2[CO_3^{2-}] + [B(OH)_4^-] + [\text{minor bases}] + [OH^-] - [H^+] \quad (3)$$

Bicarbonate and carbonate constitute roughly 98% of TA at pH 8.1.

Both physical and biological processes affect the surface water CO_2-chemistry of the oceans (Brewer, 1986; Bakker et al., 1997). DIC and TA are conservative parameters during mixing. Photosynthetic uptake of CO_2 lowers DIC and fCO_2. Biological uptake of ammonium (NH_4^+) or nitrate (NO_3^-) slightly changes TA. Precipitation of calcareous material decreases DIC and TA. Air–sea exchange of CO_2 changes the content of the inorganic carbon species in seawater, but leaves TA unaltered. The relatively slow air–sea exchange of CO_2 does not keep up with other processes acting upon the DIC components. Hence, the CO_2-content of oceanic surface waters is generally out of equilibrium with the atmospheric mixing ratio of CO_2. The observed distribution of surface water fCO_2 is strongly related to oceanic circulation in East and South Atlantic waters (Bakker et al., 1999a).

This article will relate the distribution of DIC in East Atlantic surface waters to temperature and salinity for two cruises in October–November 1993 and May–June 1994 (Table 1, Fig. 1). In two low salinity areas the inorganic carbon chemistry will be used to unravel the origin of these hydrographic features. The apparent dependence on temperature and salinity of DIC will be tested by comparing observed DIC to DIC estimated from fCO_2 and a reference value of TA normalised to salinity for different scenarios of salinity, temperature, fCO_2 and nutrient contents.

2. Methods

2.1. Meteorological and hydrographic parameters

Measurements were performed during cruises ANT XI/1 and XI/5 of R.V. *Polarstern* (Table 1,

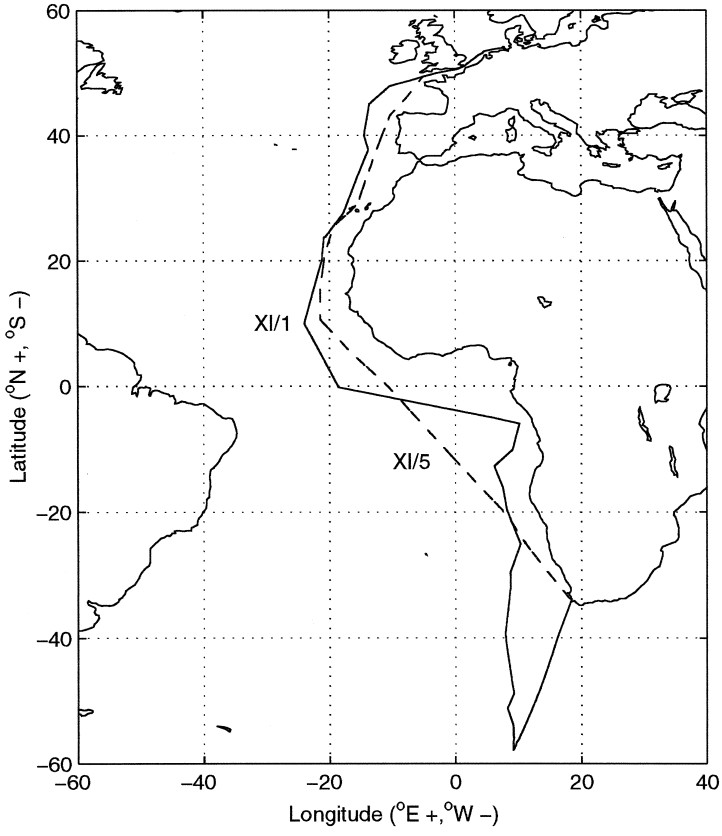

Fig. 1. Cruise tracks of the southbound cruise ANT XI/1 in October–November 1993 and of the northbound cruise ANT XI/5 in May–June 1994 of R.V. *Polarstern* in the East Atlantic Ocean (Table 1).

Fig. 1). The ship's data-acquisition system provided 10 min values for water temperature and salinity at 8 m depth, air temperature, atmospheric moisture content, atmospheric pressure at sea level, wind direction and wind speed at 10 m above sea level. Salinity is expressed on the Practical Salinity Scale.

2.2. Dissolved inorganic carbon

The content of DIC in water from 12 m depth was determined every 10 min by a coulometer (Stoll, 1994) modified for semi-continuous operation. In the extractor a subsample was acidified with 8.5% phosphoric acid (H_3PO_4) and flushed with nitrogen. The evolved CO_2 was captured in an ethanol–amine solution, which was photometrically backtitrated by the coulometer (Johnson et al., 1987). Regular calibration was performed against DIC standard seawater samples supplied by A.G. Dickson (DOE, 1994). Accuracy and precision of the coulometer were 1.5 μmol kg^{-1} (after Stoll, 1994).

2.3. The fugacity of CO_2 of water and marine air

Marine air from 20 m above sea level was pumped at a rate of 80 cm^3 s^{-1}. Seawater from 12 m depth was sprayed into an equilibrator at a rate of 40 to 50 cm^3 s^{-1} (Bakker et al., 1997). Warming of the water between sampling and the equilibrator varied from 0.1°C during ANT XI/5 to 1.5°C near the ice (XI/1). The CO_2-content of the headspace of the equilibrator and of marine air was measured with a gas chromatograph (GC) (Bakker et al., 1997). A 19-min

GC-run consisted of three calibration gases and samples for marine air and seawater. Calibration gases supplied by BOC (UK) had been calibrated against NOAA-certified standard gas mixtures. The GC had two sampling loops: one with an open outlet for sampling of calibration gases and marine air, a second as part of a closed system with the headspace of the equilibrator. CO_2 was separated from other gases and was reduced to methane (CH_4), which was detected by the flame ionisation detector (FID). At temperatures above 18°C samples were dried with silica gel.

The fugacity of CO_2 (fCO_2) in seawater was calculated from the mixing ratio of CO_2 in the headspace, atmospheric pressure, the formulae of Weiss (1974), and the temperature correction of Copin-Montégut (1988, 1989). The precision of fCO_2 in surface water was estimated as 0.7 μatm for Antarctic waters (Bakker et al., 1997). The precision of the mixing ratios of CO_2 in dry air was estimated as 0.6 μmol mol^{-1} for Antarctic regions, with an accuracy better than 0.8 μmol mol^{-1} (Bakker et al., 1997). The accuracy and precision of fCO_2 measurements in the tropical regions was lower than in Antarctic regions as a result of drying of the samples and the larger moisture correction.

2.4. Titration alkalinity

Titration alkalinity (TA) along the cruise tracks was calculated from fCO_2, DIC and interpolated values of silicate and phosphate for the definition of Dickson (1981) and the constants of Roy et al. (1993).

2.5. Fluorescence

During ANT XI/1 in situ fluorescence of seawater at 12 m depth was registered by the COMED data acquisition system (courtesy of Mr. K. Ohm, Prof. G. Krause, AWI and Dr. R. Wilkomm, University of Oldenburg). The fluorescence sensor was factory calibrated to the chlorophyll *a* content. Fluorescence of water from 8 m depth was measured with a Turner-Design TD 10 fluorometer in through-flow mode during ANT XI/5.

2.6. Nutrient contents

At regular intervals seawater from 12 m depth was sampled in duplicate. The samples were filtered across an Acrodisc 0.2 μm filter. One set of samples was stored at 2°C for determination of silicate ($Si(OH)_4$), the other was kept frozen for analysis of phosphate (as HPO_4^{2-} and $H_2PO_4^-$) and nitrate (NO_3^-). Measurements were performed one to seven weeks after sampling at the home laboratory.

3. Results

3.1. Latitudinal surface water characteristics

The cruises ANT XI/1 and XI/5 extended along the East Atlantic Ocean in October–November 1993 and May–June 1994 (Table 1, Fig. 1). The cruise tracks traversed three major hydrographic regions: the northern and the southern subtropical gyre and the Antarctic Circumpolar Current (ACC) (Fig. 2). Continental slopes were crossed at 48°N (XI/1, XI/5) and at 29°S (XI/5). The ice edge was at 57.3°S 9.2°E in November 1993 (XI/1).

A recurring latitudinal distribution was observed for surface water temperature, salinity, DIC and fCO_2 in the East Atlantic Ocean (Fig. 3). Oceanic circulation left its imprint upon the surface water CO_2-characteristics (Bakker et al., 1999a). Differences in the parameters between the two cruises partly resulted from the different cruise tracks and seasonal changes (Figs. 1 and 3). The temperature of subtropical and temperate waters was higher in autumn than in spring (Fig. 3a). Two regions, a region with low surface water salinity north of the equator and the outflow of the Congo River, displayed remarkable surface water characteristics and will be discussed in some detail.

3.1.1. Low Salinity Region

The region between 2.0° and 10.0°N (XI/1) and between 0.6° and 8.0°N (XI/5) had a pronounced minimum in salinity and a maximum in temperature and will be indicated as the Low Salinity Region (LSR) (Fig. 3). Surface water of the LSR had fCO_2

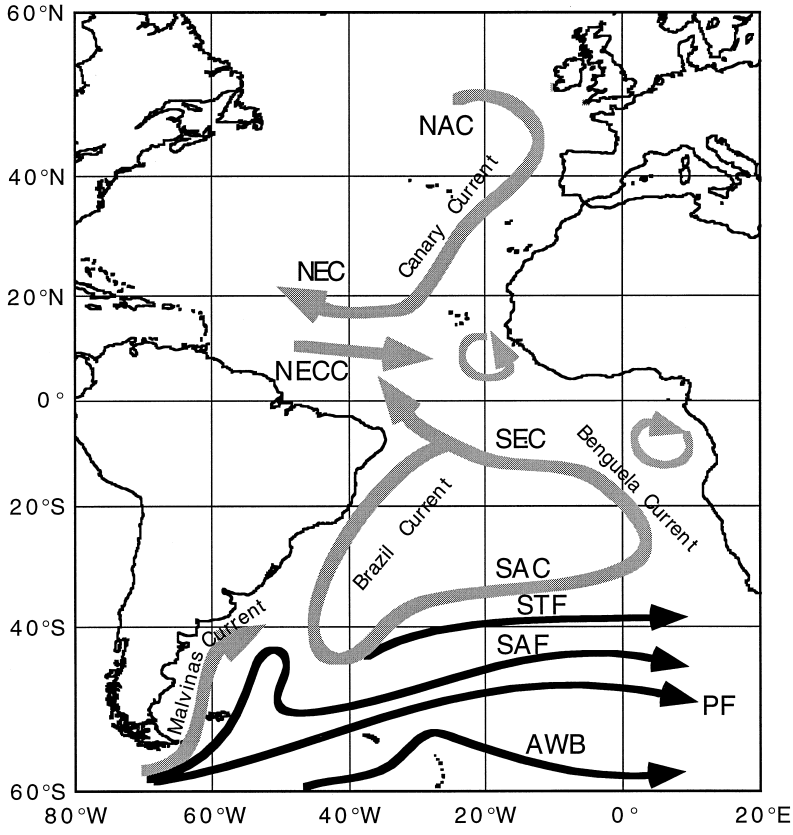

Fig. 2. Surface currents and fronts of the South and East Atlantic Ocean at a Mercator projection (after Peterson and Stramma, 1991; Schmitz, 1996). Indicated are NAC—North Atlantic Current, NEC—North Equatorial Current, NECC—North Equatorial Countercurrent, SEC—South Equatorial Current, SAC—South Atlantic Current, STF—Subtropical Front, SAF—Subantarctic Front, PF—Polar Front, and AWB—Boundary between the Antarctic Circumpolar Current and the Weddell Gyre.

below the atmospheric value, low DIC, TA, fluorescence and low nutrient contents. Strong gradients of surface water salinity, DIC, fCO_2 and TA occurred at the edges of the LSR. Similar low salinity waters with low fCO_2 were encountered in June–July 1986 (Oudot and Andrié, 1989) and in October 1995 (Lefèvre et al., 1998). They were ascribed to a combination of high precipitation and biological activity (Lefèvre et al., 1998). The observation of the LSR during several cruises in different seasons suggests that the LSR is a recurring or even a permanent feature.

The position of the LSR corresponded to that of the Intertropical Convergence Zone (ITCZ) slightly north of the equator. The southward displacement of the LSR between October 1993 (XI/1) and May–June 1994 (XI/5) followed the seasonal movement of the ITCZ. The North Equatorial Countercurrent (NECC) probably flowed eastward within the LSR. At 5.22°N 16.45°W within the LSR salinity gradually increased by 0.5 unit at a constant temperature from 0 to 40 m depth on 1 June 1994 (XI/5) (Bakker et al., 1999b). The relatively fresh water of the LSR and the shallow mixed layer had probably originated from high precipitation and low wind speed related to the ITCZ (Dessier and Donguy, 1994). Local maxima in DIC between 1.8° and 3.0°N and of fCO_2 between 8.0° and 8.2°N in May–June 1994 (XI/5) may have resulted from local upwelling.

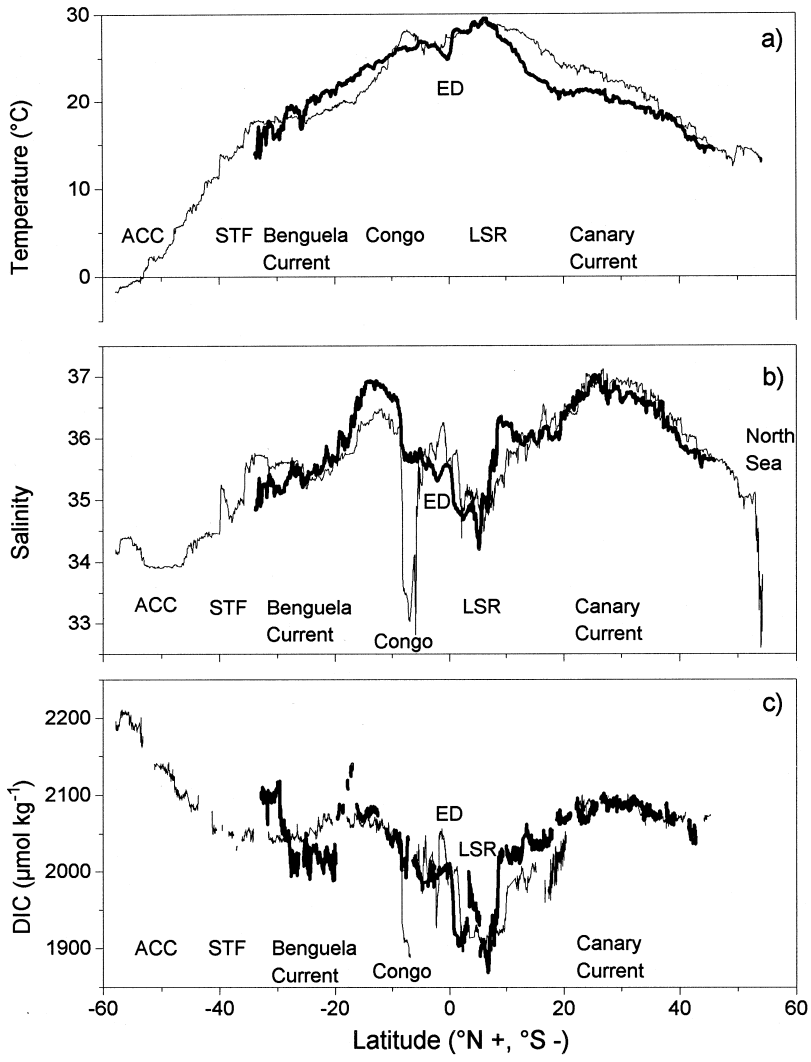

Fig. 3. The latitudinal distribution of surface water parameters for the southbound cruise ANT XI/1 (thin line, ♦) and the northbound cruise ANT XI/5 (thick line, ◇) in the East Atlantic Ocean. Parameters are temperature (a), salinity (b), dissolved inorganic carbon (DIC) (c), the difference between fCO_2 in water and air, δfCO_2(w–a) (d), the calculated titration alkalinity TA (e), 'relative chlorophyll' (XI/1) and fluorescence (XI/5) (f) and the nitrate content (NO_3^-) (g). Abbreviations are ACC—Antarctic Circumpolar Current, STF—Subtropical Front, ED—Equatorial Divergence and LSR—Low Salinity Region.

The expected effect on DIC and fCO_2 of dilution of (sub-)tropical surface water by rainwater is calculated for ANT XI/1 (Table 2). Rainwater is assumed to contain a negligible amount of DIC and TA. On the northern edge of the LSR a decrease in salinity of one unit corresponds to a calculated decrease in DIC by 55 µmol kg^{-1} and in fCO_2 by 14 µatm at a constant temperature. The change of fCO_2 by dilution is, however, counteracted by the observed, simultaneous increase in temperature by 1.9°C. Observed DIC and fCO_2 are 36 to 50 µmol kg^{-1} and 21 to 38 µatm lower than the calculated values for conservative mixing of rainwater and adjacent (sub-)tropical surface water.

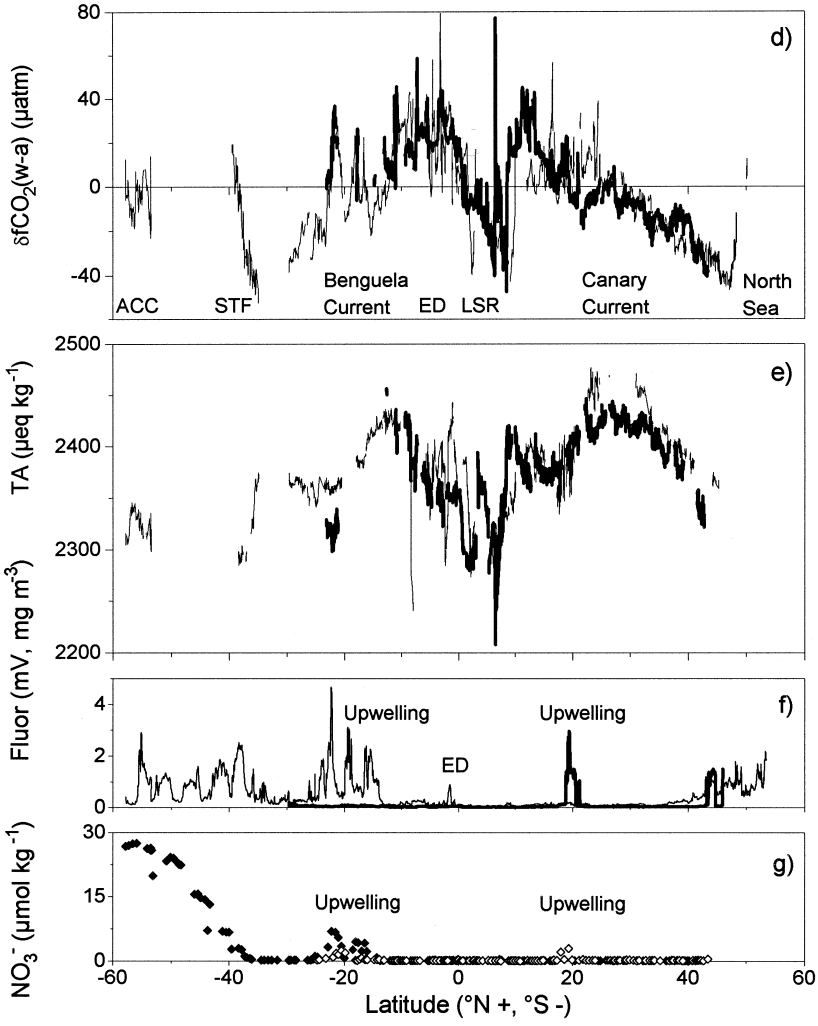

Fig. 3 (continued).

Two mixing lines with the equations:

$$\mathrm{DIC} = 99.3S - 1575 \quad (4)$$

$$\mathrm{DIC} = 95.5S - 1415 \quad (5)$$

can be distinguished between surface water in the LSR and nearby (sub-)tropical water with high salinity (Table 3, Fig. 4). The large negative offset on the *y*-axis of the mixing lines suggests that surface water in the LSR did not originate from dilution of adjacent (sub-)tropical surface water by rainwater alone.

In addition to precipitation, biological uptake of CO_2 may have lowered surface water fCO_2 and DIC in the LSR, as suggested by Lefèvre et al. (1998). Although the observed surface water fluorescence is low (Fig. 3f), ocean colour observations indicate algal blooms in a band between 5° and 10°N from late May to December (Longhurst, 1993). The temporal and spatial variability of the algal blooms follows the seasonal displacement of the NECC (Longhurst, 1993). Estimates of the annual average of the daily primary production for the eastern tropical Atlantic Ocean range from 36 to 82 mmol C m^{-2} day^{-1} (Longhurst et al., 1995; Monger et al., 1997).

Table 2
Observed surface water DIC and fCO_2 and calculated TA are compared to values estimated for conservative mixing of saline (sub-)tropical surface water and rainwater on the edges of the Low Salinity Region for ANT XI/1

Latitude	Temperature (°C)	Salinity	DIC (μmol kg^{-1})	TA (μeq kg^{-1})	fCO_2 (μatm)	DIC_{mix} (μmol kg^{-1})	TA_{mix} (μeq kg^{-1})	$fCO_{2,conT}$ (μatm)	$fCO_{2,in\ situT}$ (μatm)
15.0°N	27.04	36.10	2008.2	2395.4	353.5	–	–	–	–
9.9°N	28.40	35.62	1954.2	2364.5	324.0	1982.1	2363.5	347.2	366.1
7.5°N	28.92	35.10	1917.7	2315.5	327.7	1953.2	2329.0	339.4	365.2
1.0°S	26.15	36.22	2042.2	2423.5	360.4	–	–	–	–
0.2°S	27.35	35.61	1983.5	2368.9	347.0	2007.8	2382.7	351.0	368.0
3.0°N	28.00	35.08	1927.9	2300.2	347.6	1977.9	2347.2	342.9	368.8

For rainwater negligible contents of DIC and TA are assumed. The fCO_2 after mixing is calculated both at a constant temperature of 27.04°C for the northern edge and of 28.00°C for the southern edge ($fCO_{2,conT}$) and at in situ temperature ($fCO_{2,in\ situT}$) with the constants of Roy et al. (1993).

In the very different Antarctic ecosystem of the Polar Front a decrease of surface water fCO_2 by 1.1 to 1.4 μatm day^{-1} during 5 weeks was largely ascribed to the uptake of CO_2 by a spring bloom (Bakker et al., 1997). The corresponding primary production was 40.8 to 97.3 mmol C m^{-2} day^{-1}. Air–sea exchange of CO_2 counteracted the decrease of fCO_2 by 0.1 μatm day^{-1} for an average wind speed of 10.7 m s^{-1}. In the LSR, where wind speed is low, primary production of at least 36 mmol C m^{-2} day^{-1} may well result in a significant decrease of surface water fCO_2 and DIC.

The abrupt salinity changes on the edges of the LSR suggest that hydrographic processes supported its development and persistence. The convergence between the SEC and the NECC could have supported the strong salinity gradient on the southern boundary of the LSR. Upwelling in the Guinea Dome and along the divergence between the NECC and the NEC could have caused the observed gradients of salinity, DIC and fCO_2 on the northern edge of the LSR in June 1994 (XI/5). The LSR might represent a relatively light surface water cell bounded by downwelling on its southern edge and upwelling on its northern edge. An origin of the water of the LSR as primarily Amazon River water is unlikely, as no similar low salinity waters were observed west of 25°W during two cruises in November 1991 and February 1993 (Bakker et al., 1999a).

Strong salinity gradients of 1 to 2 units occurred on the edges of the LSR. Salinity changes of as much as 3 units were previously observed at 8°N 26°W and at 5°N 28°W in September–October 1988 (Arnault et al., 1992). Climatological maps of sea surface salinity (Tchernia, 1980; Reid, 1994; Tomczak and Godfrey, 1994) do not indicate such strong salinity gradients in the tropical Atlantic Ocean. A similar absence of a strong salinity gradient in clima-

Table 3
Linear regression between dissolved inorganic carbon (DIC) and salinity (S) in surface water with the equation $DIC = aS + b$ for the northern and southern edge of the Low Salinity Region (LSR) and the Congo-outflow for ANT XI/1

		LSR-north 7.5–15.0°N	LSR-south 1.0°S–4.0°N	Congo-outflow 5.0–10.0°S
a	(μmol kg^{-1})	99.3	95.5	54.0
b	(μmol kg^{-1})	−1575	−1415	109
r		0.97	0.99	0.96
σ_{n-1}	(μmol kg^{-1})	8.6	5.5	14.1
#		254	208	149

Symbols indicate the correlation coefficient (r), the standard deviation (σ_{n-1}) and the number of data points (#).

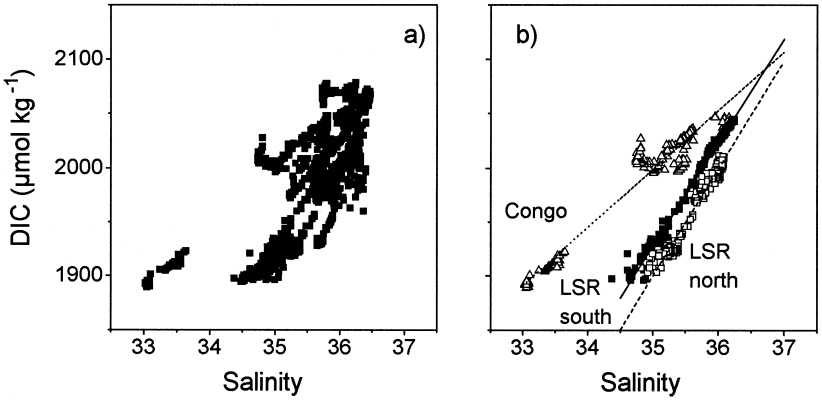

Fig. 4. (a) The surface water content of dissolved inorganic carbon (DIC) as a function of salinity between 20°N and 20°S for ANT XI/1. (b) Linear regression lines between surface water DIC and salinity for the northern edge of the Low Salinity Region (LSR) between 7.5° and 15.0°N (□), its southern edge between 1.0°S and 4.0°N (■) and the Congo-outflow between 5.0° and 10.0°S (△) (Table 3).

tological charts was noted for the convergence on the eastern edge of the Pacific Warm Pool (Picaut et al., 1996). A variable position of the salinity fronts and the smoothing effect of interpolation may explain the absence of strong salinity gradients in climatological maps.

3.1.2. Congo outflow

Water with low salinity of 33.0 to 35.6 and a low DIC-content of 1888 to 2036 µmol kg^{-1} delineated the Congo outflow between 4.7° and 8.5°S (XI/1) (Fig. 3). The black, opaque water had a high temperature of 26.2° to 27.9°C, a difference of fCO_2 across the sea surface of −4 to 43 µatm, low fluorescence and a low NO_3^--content.

A mixing line with the equation:

$$DIC = 54.0S + 109 \quad (6)$$

has been obtained between water in the Congo outflow and adjacent surface water (Table 3, Fig. 4). The relationship indicates an average DIC-content of 109 µmol kg^{-1} for the river water, neglecting changes in DIC after the water entered the ocean. This value is half of the HCO_3^--content of 220 µmol kg^{-1} for the river Congo (Probst et al., 1992). Decomposition of part of the river's total organic load of 830 µmol kg^{-1} (Nkounkou and Probst, 1987) would have increased the DIC-content, while export production would have decreased DIC.

3.2. Relationships between the surface water parameters

The complex behaviour of surface water temperature, salinity, DIC, fCO_2 and TA was examined in order to identify functional relationships between the parameters.

3.2.1. Temperature and salinity

The relationship between temperature and salinity changed from the equator towards the poles (Fig. 5a). Maximum temperatures occurred in two regions with relatively low salinity: the LSR and the Congo outflow. Highest salinity was observed at temperatures of 22–26°C in subtropical waters. Salinity and temperature decreased from subtropical areas towards temperate and subantarctic regions in a distinct band for each hemisphere. Surface water of the North Sea had low salinity and a temperature of 12–14°C.

3.2.2. The dependence of DIC on salinity and temperature

Individual regions of the East Atlantic Ocean had a distinct behaviour of DIC relative to salinity and

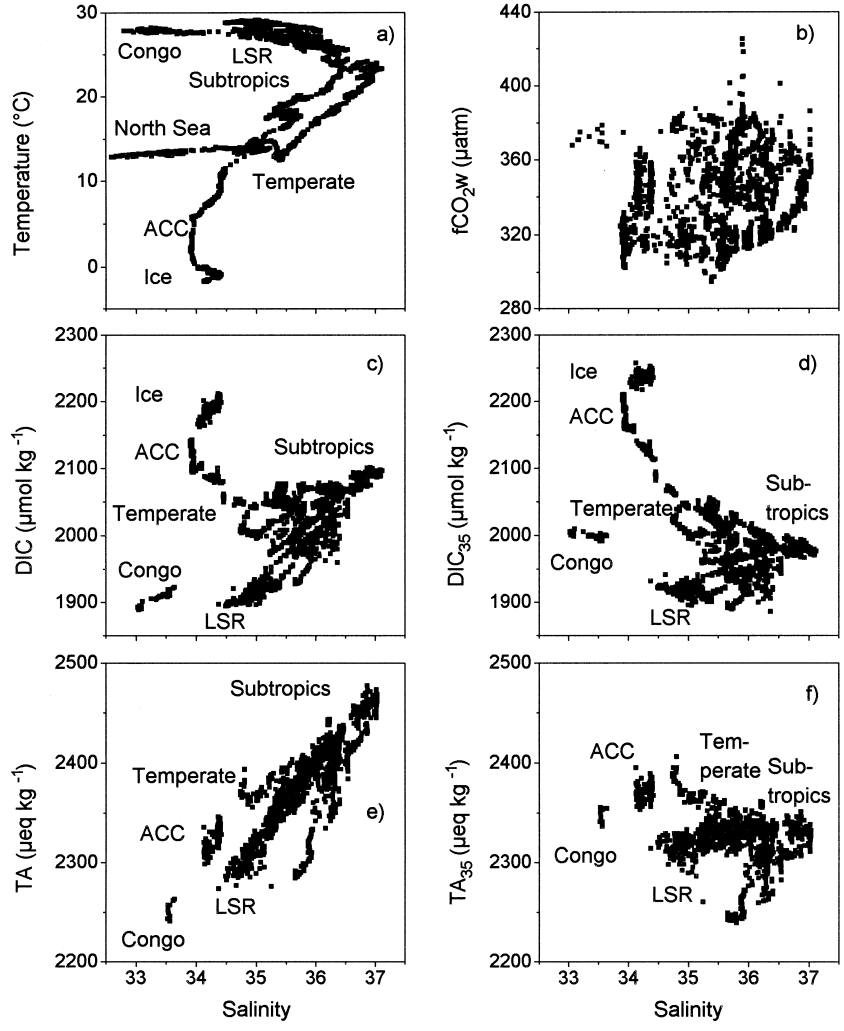

Fig. 5. Surface water values as a function of salinity for the cruise ANT XI/1 in October–November 1993 in the East Atlantic Ocean. Parameters are temperature (a), fCO_2 (b), dissolved inorganic carbon (DIC) (c), DIC normalised to a salinity of 35 (d), calculated titration alkalinity (TA) (e), and TA normalised to a salinity of 35 (TA_{35}) (f). Abbreviations are ACC—Antarctic Circumpolar Current and LSR—Low Salinity Region. 'Temperate' denotes temperate waters. 'Ice' indicates the presence of sea ice.

temperature (Fig. 5c, Fig. 6c). Surface water DIC increased as salinity increased and temperature slightly decreased from the LSR to adjacent (sub-) tropical waters. DIC normalised to a salinity of 35 (DIC_{35}) was almost independent of salinity for these waters (Fig. 5d). This suggested a dependence of DIC on salinity from the LSR to adjacent waters.

From subtropical to temperate waters DIC was relatively constant for decreasing temperature and salinity, while DIC_{35} showed a linear increase with both parameters (Fig. 5c–d, Fig. 6c–d). The effects of temperature and salinity changes on DIC apparently counteracted each other in these waters.

From temperate to Antarctic waters the increase of DIC was opposed to the decrease of temperature and salinity (Fig. 5c, Fig. 6c). The decrease of temperature and salinity enhanced the solubility of CO_2 and shifted the carbonate equilibria,

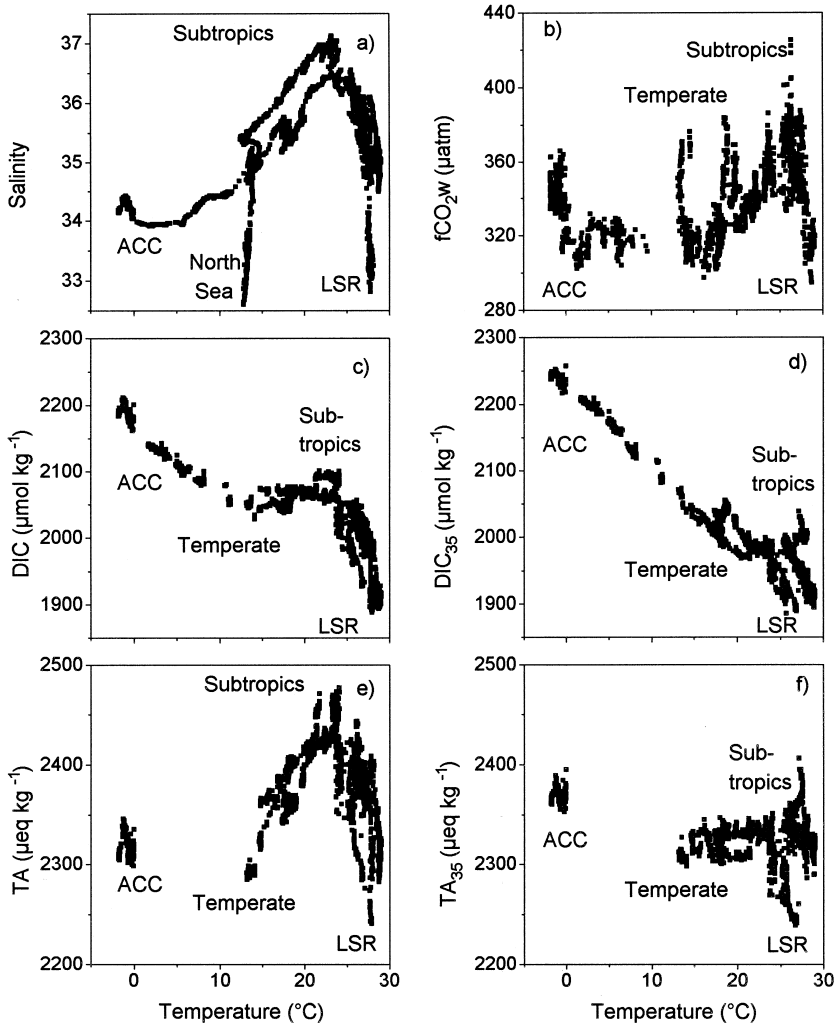

Fig. 6. Surface water values as a function of temperature for the cruise ANT XI/1 in October–November 1993 in the East Atlantic Ocean. Parameters are salinity (a), fCO_2 (b), dissolved inorganic carbon (DIC) (c), DIC normalised to a salinity of 35 (d), calculated titration alkalinity (TA) (e), and TA normalised to a salinity of 35 (TA_{35}) (f). Abbreviations are ACC—Antarctic Circumpolar Current and LSR—Low Salinity Region. 'Temperate' denotes temperate waters.

which promoted the increase of DIC towards colder waters.

3.2.3. The relationship between fCO_2, temperature, salinity and DIC

Surface water fCO_2 was independent of salinity (Fig. 5b). The dependence of fCO_2 on temperature and DIC varied for the oceanic regions (Bakker et al., 1999a) (Fig. 6b, Fig. 7a).

3.2.4. The dependence of TA on temperature and salinity

The linear relationship between TA and salinity (Fig. 5e) disappeared by normalising TA to a salinity of 35 (TA_{35}) (Fig. 5f). This indicated a highly conservative behaviour of TA for most of the research area and explained the resemblance between the figures of salinity and TA against temperature (Fig. 6a and e). Processes, such as precipitation and dissolution of calcareous material, biological uptake

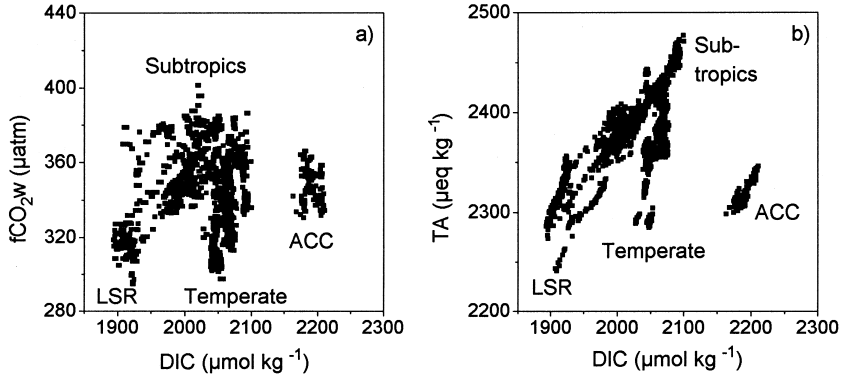

Fig. 7. Surface water values of the fugacity of CO_2 (fCO_2) (a), and calculated titration alkalinity (TA) (b), as a function of dissolved inorganic carbon (DIC) for the cruise ANT XI/1 in the East Atlantic Ocean in October–November 1993. Abbreviations are ACC—Antarctic Circumpolar Current and LSR—Low Salinity Region. 'Temperate' denotes temperate waters.

of nitrogen components and mixing in of water, apparently did not greatly affect TA normalised to a salinity of 35. TA_{35} was relatively independent of temperature except in tropical waters (Fig. 6f).

4. Discussion

4.1. Scenarios that estimate DIC from salinity and temperature

The above suggests that the spatial variability of DIC along the eastern boundary of the Atlantic Ocean was related to both temperature and salinity, while TA was primarily affected by salinity. The dependence of surface water DIC on temperature and salinity is studied by comparing observed DIC to DIC estimated for different scenarios of temperature and salinity (Table 4). With these scenarios surface water DIC was calculated along the cruise tracks from fCO_2 and a reference value of TA and nutrient contents normalised to salinity (TA_S, $PO_{4,S}^{3-}$, $Si(OH)_{4,S}$). The latter values of TA and the nutrient contents were obtained for each data point by multiplying their reference value (TA_{ref}, $PO_{4,ref}^{3-}$, $Si(OH)_{4,ref}$) with the ratio of salinity (S) to the reference salinity (S_{ref}):

$$TA_S = TA_{ref} S/S_{ref} \quad (7)$$

The use of a reference value for TA does not take into account the mixing in of water with a different ratio of TA relative to salinity and biological changes of TA. The constants of Roy et al. (1993) are applied.

Reference points were chosen at 26.4°N 18.6°W (XI/1) and at 26.4°N 18.3°W (XI/5) (Table 5). Surface water characteristics of the reference points are referred to as 'reference values'. Reference val-

Table 4
Scenarios A to E for the calculation of the surface water content of dissolved inorganic carbon (DIC) from the fugacity of CO_2 (fCO_2) and titration alkalinity (TA) normalised to salinity

Scenario	Temperature	Salinity	fCO_2	TA	PO_4^{3-}	$Si(OH)_4$
A	In situ	S_{ref}	$xCO_{2,air}$	TA_{ref}	$PO_{4,ref}^{3-}$	$Si(OH)_{4,ref}$
B	T_{ref}	In situ	$xCO_{2,air}$	TA_S	$PO_{4,S}^{3-}$	$Si(OH)_{4,S}$
C	In situ	In situ	$xCO_{2,air}$	TA_S	$PO_{4,S}^{3-}$	$Si(OH)_{4,S}$
D	In situ	In situ	In situ	TA_S	$PO_{4,S}^{3-}$	$Si(OH)_{4,S}$
E	In situ	In situ	In situ	TA_S	In situ	In situ

The subscript 'ref' denotes a value at the reference point at 26.4°N (Table 5). The subscript 'S' indicates a reference value normalised to in situ salinity along the cruise tracks (Eq. (7)). Either surface water fCO_2 in equilibrium with a constant mixing ratio of CO_2 in dry air ($xCO_{2,air}$) or in situ fCO_2 is used.

Table 5
Surface water values for temperature, salinity, DIC, TA, the difference in fCO_2 between water and air (δfCO_2(w–a)), phosphate (PO_4^{3-}) and silicate ($Si(OH)_4$) at the reference points for ANT XI/1 and XI/5

Cruise	ANT XI/1	ANT XI/5
Latitude (°N)	26.4	26.4
Longitude (°W)	18.6	18.3
DIC (μmol kg^{-1})	2090	2095
Temperature (°C)	23.31	20.93
Salinity, *S*	36.84	36.80
TA (μeq kg^{-1})	2468	2440
$xCO_{2,air}$ (μmol mol^{-1})	356.0	360.0
δfCO_2(w–a) (μatm)	7.1	0.3
PO_4^{3-} (μmol kg^{-1})	0.0	0.1
$Si(OH)_4$ (μmol kg^{-1})	0.4	0.7

The mixing ratio of CO_2 in dry air ($xCO_{2,air}$) is also given. Reference values are used to calculate DIC with scenarios A to E (Table 4).

ues were similar for both cruises, except temperature, which decreased by 2.3°C between the cruises. Relatively similar values of DIC, fCO_2 and salinity at a lower temperature indicate a change of the surface water CO_2-characteristics at the reference point between cruises. Changes in the CO_2-system could have taken place by horizontal advection, upwelling, mixing and/or biological activity.

Surface water fCO_2 was close to equilibrium with the atmospheric value at the reference points. In scenarios A to C surface water fCO_2 is assumed to be in equilibrium with a constant mixing ratio of CO_2 in dry air ($xCO_{2,air}$) of 356 μmol mol^{-1} (XI/1) and of 360 μmol mol^{-1} (XI/5) (Tables 4 and 5). The accuracy of the scenarios is obtained as the average of the absolute differences between observed and estimated DIC along the cruise tracks (Table 6).

4.2. Scenarios for ANT XI / 1

DIC-values with the scenarios A to E are compared below to the observed values for ANT XI/1 (Tables 4 and 6, Fig. 8). Obviously all scenarios yield a good fit at the reference point, where in situ values are used for temperature, salinity, TA and the nutrient contents, and where surface water fCO_2 is close to equilibrium with the applied atmospheric mixing ratio of CO_2.

4.2.1. Scenario A

Scenario A estimates DIC from in situ temperature, constant reference values of salinity, TA, PO_4^{3-} and $Si(OH)_4$ and constant $xCO_{2,air}$ (Table 4). DIC as a function of in situ temperature changes by air–sea exchange, as surface water fCO_2 is forced to be in equilibrium with a constant atmospheric CO_2-content. With this scenario DIC increases from high to low temperatures.

Scenario A reproduces the observed general trend of low DIC near the equator, higher values in temperate waters and highest DIC in the Southern Ocean (Fig. 8a). The DIC-content of East Atlantic surface waters is clearly influenced by temperature. However, large deviations exist between estimated and observed values with an average absolute difference of 83 μmol kg^{-1} (Table 6).

4.2.2. Scenario B

Scenario B obtains DIC for in situ salinity, constant temperature and $xCO_{2,air}$. The reference values of TA and the nutrient contents are normalised to in situ salinity (Table 4). With this scenario the effects of precipitation, evaporation and river input on DIC are simulated, although the TA-content of freshwater sources is neglected.

Table 6
The accuracy, standard deviation (σ_{n-1}) and number of data points for the fits of dissolved inorganic carbon (DIC) in surface water with the scenarios A to E for cruises ANT XI/1 and XI/5 (Table 4)

Cruise		Scenario				
		A	B	C	D	E
XI/1	Accuracy (μmol kg^{-1})	83	61	22	17	18
	σ_{n-1} (μmol kg^{-1})	48	67	17	13	13
	Number	3673	3673	3673	2895	2895
XI/5	Accuracy (μmol kg^{-1})	45	31	20	15	14
	σ_{n-1} (μmol kg^{-1})	34	29	14	12	12
	Number	3140	3140	3140	2182	2182
XI/5′	Accuracy (μmol kg^{-1})	64	30	28	30	30
	σ_{n-1} (μmol kg^{-1})	36	29	17	12	12
	Number	3140	3140	3140	2182	2182

The accuracy has been derived as the average absolute difference between the observed and the estimated values. For ANT XI/5 the procedure has been repeated using reference values of ANT XI/1 (XI/5′).

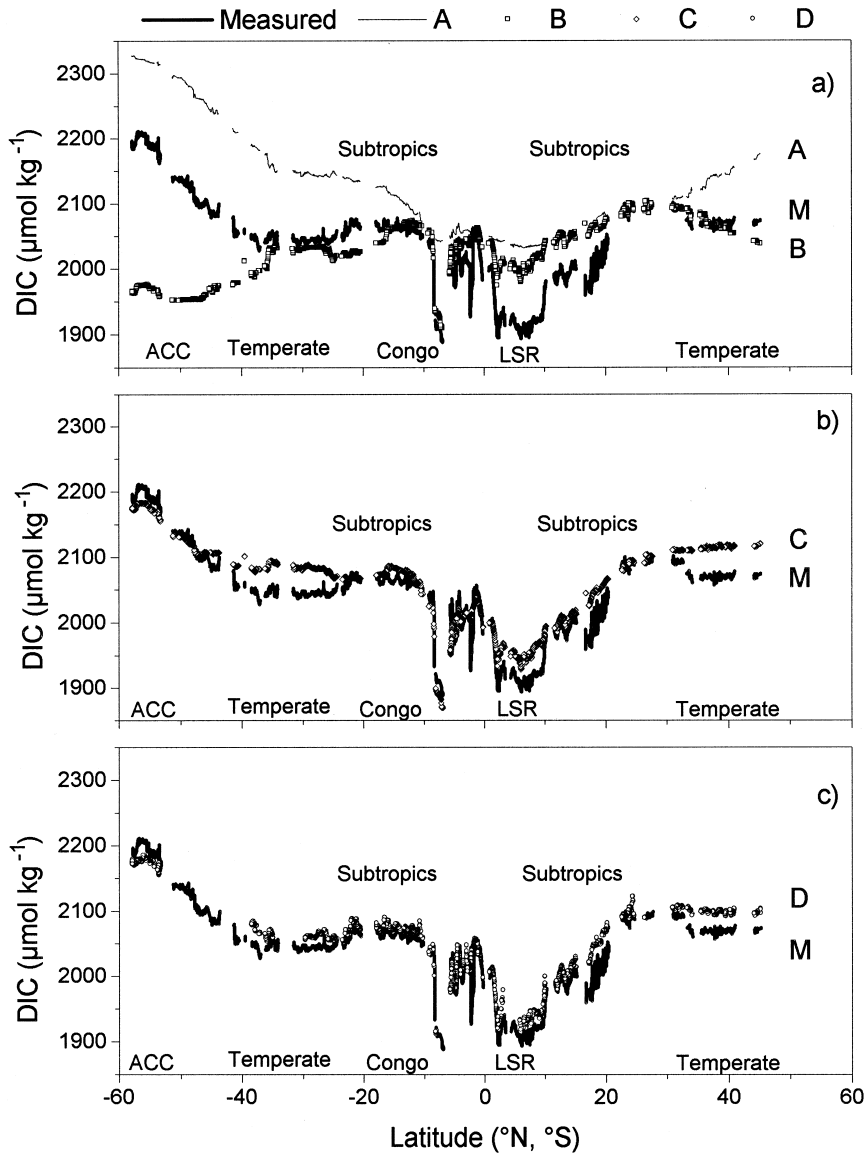

Fig. 8. The latitudinal distribution of measured (M) and estimated dissolved inorganic carbon (DIC) in surface water with scenarios A, B (a), C (b) and D (c) for cruise ANT XI/1 in October–November 1993 in the East Atlantic Ocean. The graph for scenario E strongly resembles that for scenario D and is not shown. Abbreviations are ACC—Antarctic Circumpolar Current and LSR—Low Salinity Region. 'Temperate' denotes temperate waters.

Estimated and observed DIC display the same trends in subtropical and tropical waters for scenario B (Fig. 8a). High DIC is estimated for (sub-)tropical waters with high salinity. Relatively low DIC is predicted for the LSR and the Congo outflow. From temperate to polar waters the similarity between the estimated and the observed pattern gradually breaks down. The above suggests that salinity strongly affects DIC in subtropical and tropical surface waters.

4.2.3. Scenario C

Scenario C estimates DIC for in situ temperature, in situ salinity and constant $xCO_{2,air}$. Reference values of TA and the nutrient contents are normalised to in situ salinity (Table 4).

The patterns of estimated and observed DIC have a general resemblance (Fig. 8b). Clearly this scenario yields a better fit of the observed DIC-values than the scenarios A and B, which estimated DIC from either in situ temperature or in situ salinity (Table 6, Fig. 8a–b). Estimated DIC according to scenario C has an accuracy of 22 μmol kg^{-1} with a standard deviation (σ_{n-1}) of 17 μmol kg^{-1} (Table 6). Large differences between observed and estimated DIC exist in three areas with surface water fCO_2 well below the atmospheric value, notably the northern temperate waters, the LSR and the southern temperate waters.

4.2.4. Scenario D

Scenario D calculates DIC for in situ temperature, salinity and fCO_2. Reference values of TA and the nutrient contents are normalised to in situ salinity (Table 4).

Use of in situ fCO_2 decreases the difference between observed and estimated DIC in the three areas with low surface water fCO_2, that exhibit a large difference for scenario C (Fig. 8b–c). It improves the accuracy to 17 μmol kg^{-1} (σ_{n-1} of 13 μmol kg^{-1}) (Table 6).

4.2.5. Scenario E

Scenario E uses in situ temperature, salinity, fCO_2 and nutrient contents. The use of in situ nutrient contents does not significantly improve the accuracy of the estimated DIC-values relative to scenario D (Table 6). This is not surprising, as nutrient contents were low in most of the research area (Fig. 3g) and as nutrients only have a slight effect on TA. The graph for scenario E strongly resembles that for scenario D and is not shown.

4.3. Scenarios for ANT XI/5

Repetition of the above procedure for ANT XI/5 produces similar results (Tables 4 and 6, Fig. 9). Use of either in situ temperature (scenario A) or in situ salinity (scenario B) describes part of the observed latitudinal distribution of DIC. The combination of in situ temperature and in situ salinity (scenario C) gives a better approximation of the observed values with an accuracy of 20 μmol kg^{-1} (σ_{n-1} of 14 μmol kg^{-1}). Introduction of in situ fCO_2 improves the accuracy to 15 μmol kg^{-1}. The use of in situ nutrient values in the evaluation does not yield a significantly better fit. The accuracy of the fits is similar for both cruises (Table 6).

4.4. Scenarios for ANT XI/5 with reference values from ANT XI/1

Between cruises temperature decreased by 2.3°C at the reference point, while other parameters remained constant (Table 5). Consequently, a different TA is calculated at the reference point for both cruises. The effect of a different reference value for TA is studied by repeating the calculation of DIC with the scenarios A to E for ANT XI/5 with reference values of ANT XI/1 (Table 5). The fit XI/5′ has a large offset relative to the observed DIC-values in northern subtropical surface waters. Elsewhere the fit is of a similar quality to the earlier fit. The large offset results in an overall fit (XI/5′) with less accuracy than the original fit for ANT XI/5 (Table 6).

4.5. Evaluation of the scenarios

The distribution of DIC according to scenario C corresponds relatively well to the observed values in the tropical and subtropical regions (Fig. 8b, Fig. 9b). The quality of the fits does not change, when passing from the northern subtropical gyre to the southern one. The observed decrease of DIC from subtropical to temperate waters is described better by scenario D, which utilises in situ fCO_2 (Figs. 8 and 9). The estimated and the observed pattern of DIC resemble each other in Antarctic waters (Fig. 8b).

4.5.1. Low Salinity Region

DIC estimated using in situ salinity in scenario B exhibits a minimum similar in appearance to the one observed in the LSR (Fig. 8a, Fig. 9a). The use of both in situ temperature and in situ salinity (scenario

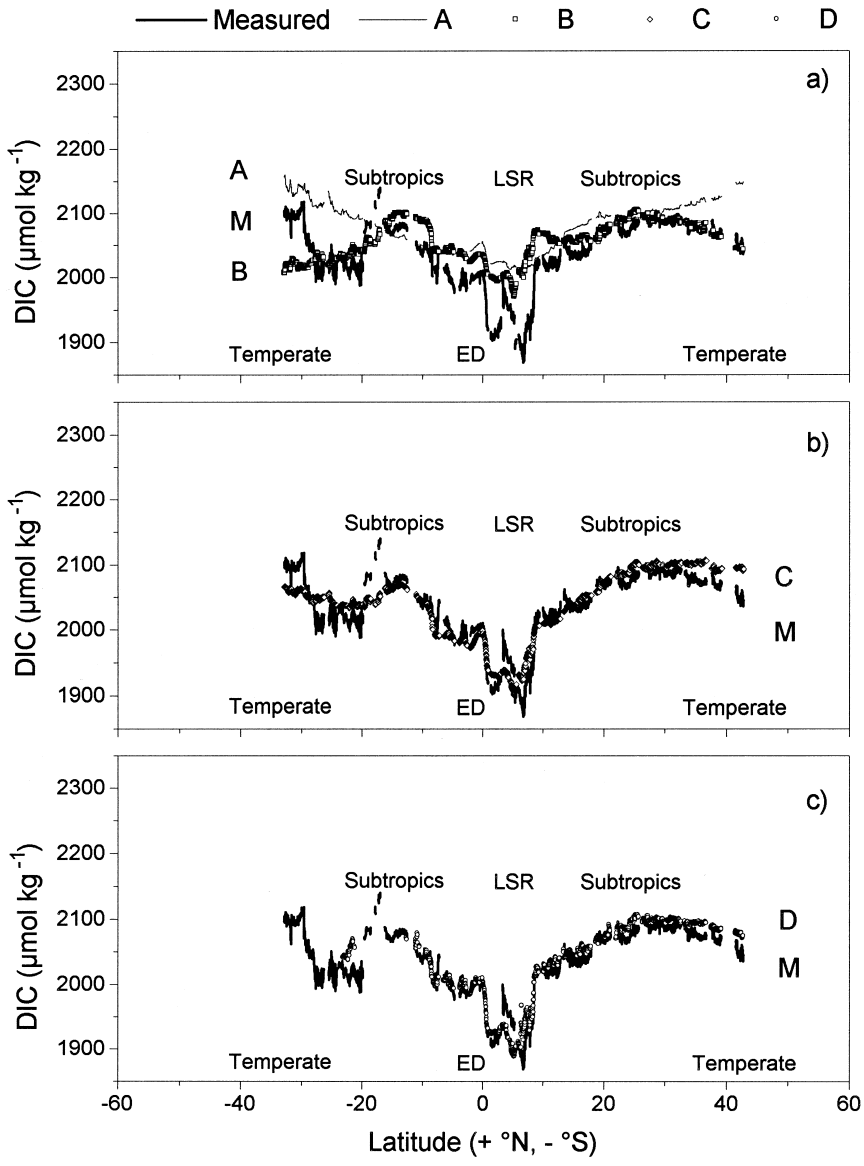

Fig. 9. The latitudinal distribution of measured (M) and estimated dissolved inorganic carbon (DIC) in surface water with scenarios A, B (a), C (b) and D (c) for cruise ANT XI/5 in the East Atlantic Ocean in May–June 1994. The graph for scenario E strongly resembles that for scenario D and is not shown. Abbreviations are LSR—Low Salinity Region and ED—Equatorial Divergence. 'Temperate' denotes temperate waters.

C) improves the fit for the abrupt DIC-changes at the edges of the LSR (Fig. 8b, Fig. 9b). This suggests that both high rainfall and high temperature promote the DIC-minimum in the LSR. Use of in situ fCO_2 (scenario D) further improves the fit of DIC in the LSR.

Only a small part of the observed maximum in DIC between 1.8° and 3.0°N within the LSR is estimated with scenarios B to E for ANT XI/5 (Fig. 9b). Apparently dilution of seawater by a variable amount of rainwater does not explain this maximum in DIC. Local upwelling of water with a TA nor-

malised to salinity different from the reference value may have promoted these elevated DIC-values.

4.5.2. Congo outflow

DIC in the Congo outflow is relatively well described with scenarios B and C (XI/1) (Fig. 8a–b). Either river water had TA close to zero, which is an implicit assumption of these scenarios, or biological changes of DIC counteracted the effect of river water TA higher than zero on estimated DIC.

4.5.3. Coastal upwelling

Scenario C does not reproduce the observed high DIC-contents south of 28°S and between 16° and 18°S (XI/5) (Fig. 9b). As coastal upwelling occurred in these regions, the offset of the scenario relative to the observations may indicate that the upwelled water had a TA normalised to salinity different from the reference value.

5. Conclusions

Two case studies in low salinity regions have demonstrated the use of the inorganic carbon chemistry as a means of unravelling the origin of hydrographic features. A region with surface water fCO_2 below the atmospheric value and low salinity and DIC was observed north of the equator. As the position of the region corresponded to that of the Intertropical Convergence Zone, dilution of (sub-) tropical surface water by rainwater was considered as a potential mechanism for the low surface water values in the LSR. Regression lines between surface water DIC and salinity for the northern and southern edges of the LSR had a large negative offset. Estimated DIC and fCO_2 for conservative mixing of adjacent (sub-)tropical surface water with rainwater were much higher than the observed values of DIC and fCO_2 in the LSR. Both the negative offset of the regression lines and the calculation for conservative dilution by rainwater demonstrated that dilution by rainwater did to some extent, but not completely explain the low observed values of DIC and fCO_2. Biological uptake of CO_2 may have further lowered DIC and fCO_2 in the LSR.

Low surface water salinity and DIC delineated the Congo outflow. A regression line between DIC and salinity suggested a DIC-content of 109 μmol kg^{-1} for the river water, neglecting DIC-changes after the water entered the ocean. This value corresponds relatively well to a HCO_3^--content of 220 μmol kg^{-1} for the river Congo (Probst et al., 1992).

The TA is primarily influenced by salinity in East Atlantic surface waters. The dependence of DIC on temperature and salinity was tested by comparing observed DIC to values calculated for different scenarios of temperature and salinity. Changes of DIC were found to be related to both temperature and salinity. Surface water DIC was estimated along the cruise tracks with an accuracy of 22 μmol kg^{-1} and a standard deviation (σ_{n-1}) of 17 μmol kg^{-1} from in situ temperature, in situ salinity, constant xCO_2 and reference values of TA and nutrient contents normalised to salinity (scenario C) (Table 6). The accuracy was improved to 17 μmol kg^{-1} (σ_{n-1} of 13 μmol kg^{-1}) by use of in situ surface water fCO_2 with the main improvements in areas with fCO_2 well below the atmospheric value. The above procedure of scenario validation is a powerful diagnostic tool to assess causes of the spatial variability of DIC in surface water. The relatively good agreement between observed and estimated DIC is probably restricted to regions with low biological activity and little mixing in of water with a different TA normalised to salinity relative to the water under consideration.

Acknowledgements

We are grateful to the Alfred Wegener Institute for Polar and Marine Research (AWI) for making R.V. *Polarstern* available to us. Captain, crew and scientists created a good working atmosphere. Rainer Wilkomm (Fachbereich Physik, University of Oldenburg), Klaus Ohm and Günther Krause (AWI) kindly provided the COMED data. Erica Koning calibrated the CO_2-standards. Karel Bakker and Jan van Ooijen (Marine Chemistry and Geology, Netherlands Institute for Sea Research, NIOZ) performed the nutrient analyses. Useful comments by David Turner (University of Göteborg) and two anonymous reviewers helped to improve the manuscript. The Dutch National Research Programme on Global Air Pollution and Climate Change and The Netherlands Geosciences Foundation supported the research. This is NIOZ publication 3192.

References

Arnault, S., Goudreau, L., Menard, Y., 1992. Comparison of the altimetric signal with in situ measurements in the tropical Atlantic Ocean. Deep-Sea Res. 39, 481–499.

Bakker, D.C.E., de Baar, H.J.W., Bathmann, U.V., 1997. Changes of carbon dioxide in Surface waters during spring in the Southern Ocean. Deep-Sea Res. II 44, 91–128.

Bakker, D.C.E., de Baar, H.J.W., de Jong, E., 1999a. The Atlantic Ocean: an overall sink for atmospheric CO_2 with a strong imprint of oceanic circulation. Submitted.

Bakker, D.C.E., de Baar, H.J.W., de Jong, E., 1999b. Dissolved carbon dioxide in tropical East Atlantic surface waters. Phys. Chem. Earth, in press.

Brewer, P.G., 1986. What controls the variability of carbon dioxide in the surface ocean? A plea for complete information. In: Burton, J.D., Brewer, P.G., Chesselet, R. (Eds.), Dynamic Processes in the Chemistry of the Upper Ocean. Plenum, New York.

Copin-Montégut, C., 1988. A new formula for the effect of temperature on the partial pressure of CO_2 in seawater. Mar. Chem. 25, 29–37.

Copin-Montégut, C., 1989. Corrigendum. A new formula for the effect of temperature on the partial pressure of CO_2 in seawater. Mar. Chem. 27, 143–144.

Dessier, A., Donguy, J.R., 1994. The sea surface salinity in the tropical Atlantic between 10°S and 30°N—seasonal and interannual variations (1977–1989). Deep-Sea Res. I 41, 81–100.

Dickson, A.G., 1981. An exact definition of total alkalinity and a procedure for the estimation of alkalinity and total inorganic carbon from titration data. Deep-Sea Res. 28, 609–623.

DOE, 1994. In: Dickson, A.G., Goyet, C. (Eds.), Handbook of Methods for the Analysis of the Various Parameters of the Carbon System in Sea Water, version 2, ORNL/CDIAC, p. 74.

Houghton, J.T., Meira Filho, L.G., Callander, B.A., Harris, N., Kattenberg, A., Maskell, K. (Eds.), 1996. Climate Change 1995—The Science of Climate Change: Contribution of Working Group I to the Second Assessment Report of the Intergovernmental Panel on Climate Change. Cambridge Univ. Press, Cambridge.

Johnson, K.M., Williams, P.J.LeB., Brändström, L., Sieburth, J.McN., 1987. Coulometric total carbon dioxide analysis for marine studies: automatization and calibration. Mar. Chem. 21, 117–133.

Lefèvre, N., Moore, G., Aiken, J., Watson, A.J., Cooper, D., 1998. Variability of pCO_2 in the tropical Atlantic in 1995. J. Geophys. Res. 103, 5623–5634.

Longhurst, A., 1993. Seasonal cooling and blooming in tropical oceans. Deep-Sea Res. I 40, 2145–2165.

Longhurst, A., Sathyendranath, S., Platt, T., Caverhill, C., 1995. An estimation of global primary production in the ocean from satellite radiometer data. J. Plankton Res. 17, 1245–1271.

Monger, B., McClain, C., Murtugudde, R., 1997. Seasonal phytoplankton dynamics in the eastern tropical Atlantic. J. Geophys. Res. 102 (C6), 12389–12411.

Nkounkou, R.R., Probst, J.L., 1987. Hydrology and geochemistry of the Congo river system. In: Degens, E.T., Kempe, S., Wei-Bin G. (Eds.), Transport of Carbon and Minerals in Major World Rivers, Part 4. Mitt. Geol.-Paläont. Inst. Uni. Hamburg, SCOPE/UNEP 64, 483–508.

Oudot, C., Andrié, C., 1989. Short term changes in the partial pressure of CO_2 in eastern tropical Atlantic surface seawater and in atmospheric CO_2 mole fraction. Tellus 41B, 537–553.

Peterson, R.G., Stramma, L., 1991. Upper-level circulation in the South Atlantic Ocean. Prog. Oceanogr. 26, 1–73.

Picaut, J., Ioualalen, M., Menkes, C., Delcroix, T., McPhaden, M.J., 1996. Mechanism of the zonal displacements of the Pacific Warm Pool: implications for ENSO. Science 274, 1486–1489.

Poisson, A., Metzl, N., Brunet, C., Schauer, B., Bres, B., Ruiz-Pino, D., Louanchi, F., 1993. Variability of sources and sinks of CO_2 in the western Indian and Southern Oceans during the year 1991. J. Geophys. Res. 98, 22759–22778.

Probst, J.-L., Nkounkou, R.R., Krempp, G., Bricquet, J.P., Thibaux, J.P., Olivry, J.L., 1992. Dissolved major elements exported by the Congo and the Ubangui rivers during the period 1987–1989. J. Hydrol. 135, 237–257.

Reid, J.L., 1994. On the total geostrophic circulation of the North Atlantic Ocean: flow patterns, tracers and transports. Prog. Oceanogr. 33, 1–92.

Roy, R.N., Roy, L.N., Vogel, K.M., Porter-Moore, C., Pearson, T., Good, C.E., Millero, F.J., Campbell, D.M., 1993. The dissociation constants of carbonic acid in seawater at salinities 5 to 45 and temperatures 0 to 45°C. Mar. Chem. 44, 249–267.

Schmitz, W.J., 1996. On the eddy field in the Aghullas retroflection with some global considerations. J. Geophys. Res. 101, 16259–16271.

Stoll, M.H.C., 1994. Inorganic carbon behaviour in the North Atlantic Ocean. Thesis Rijksuniversiteit Groningen, Groningen.

Sverdrup, H.U., Johnson, M.W., Fleming, R.H., 1942. The Oceans: Their Physics, Chemistry and General Biology. Prentice-Hall, 1087 pp.

Takahashi, T., Olafsson, J., Goddard, J.G., Chipman, D.W., Sutherland, S.C., 1993. Seasonal variation of CO_2 and nutrients in the high-latitude surface oceans: a comparative study. Global Biogeochem. Cycles 7, 843–878.

Takahashi, T., Feely, R.A., Weiss, R.F., Wanninkhof, R.H., Chipman, D.W., Sutherland, S.C., Takahashi, T.T., 1997. Global air–sea flux of CO_2: an estimate based on measurements of sea–air pCO_2 difference. Proc. Natl. Acad. Sci. 94, 8292–8299.

Tchernia, P., 1980. Descriptive Physical Oceanography. Pergamon Marine Series 3. Pergamon, Oxford.

Tomczak, M., Godfrey, J.S., 1994. Regional Oceanography: An Introduction. Pergamon.

Weiss, R.F., 1974. Carbon dioxide in water and seawater: the solubility of a non-ideal gas. Mar. Chem. 2, 203–205.